HIV antiretrovirals have differential effects on viability and function in human iPSC-derived neurons and neural precursor cells

Alyson S. Smith[1], Soneela Ankam[1], Ranor C.B. Basa[1], Kara L. Gordon[1], Alexey V. Terskikh[2], Kelly L. Jordan-Sciutto[3,4], Jeffrey Price[1,5], Patrick M. McDonough[1]

[1]Vala Sciences, Inc., San Diego, CA; [2]Sanford Burnham Prebys Medical Discovery Institute, La Jolla, CA; [3]Department of Pathology, Perelman School of Medicine, University of Pennsylvania, Philadelphia, PA; [4]Department of Basic and Translational Sciences, School of Dental Medicine, University of Pennsylvania, Philadelphia, PA; [5]Scintillon Institute, San Diego, CA

To whom correspondence should be addressed: asmith@valasciences.com

Abstract

Combination antiretroviral therapy (cART) improves life expectancy and lowers the incidence of central nervous system (CNS) opportunistic infections, lymphomas, and HIV-associated dementia in HIV+ people. However, mild-to-moderate HIV-associated neurocognitive disorders (HAND) persist in about 50% of HIV+ people, even when HIV replication is well controlled. In vitro, animal model, and clinical studies suggest that cART neurotoxicity could be a contributing factor to the progression of HAND. In this study, we developed two in vitro model systems using glutamatergic neurons derived from human induced pluripotent stem cells (hiPSC-Gluts) and fetal neural precursor cells (hNPCs) to assay for antiretroviral (ARV) effects on mature and developing neurons, respectively. We tested four ARVs: the nucleoside/nucleotide reverse transcriptase inhibitors tenofovir disproxil fumarate (TDF) and emtricitabine (FTC) and the integrase inhibitors dolutegravir (DTG) and elvitegravir (EVG). DTG, EVG, and TDF decreased hiPSC-Glut viability and neurite length; all four antiretrovirals decreased hiPSC-Glut synapse counts; and DTG and EVG decreased the frequency and magnitude of hiPSC-Glut calcium transients. The magnitude of these neurotoxic effects increased with longer ARV exposure times and with the exposure of hiPSC-Gluts to two or three ARVs simultaneously. These results suggest that certain ARVs could cause HAND by decreasing the survival and function of CNS neurons. In fetal hNPCs, TDF decreased viability and changed the distribution of epigenetic histone modifications, suggesting that this ARV may alter neurogenesis, which could impair cognition in adults and/or CNS development for those exposed to ARV in utero or early childhood. Our study establishes human preclinical neurotoxicity systems that can screen for potential ARV CNS toxicity and develop safer cART regimens.

Introduction:

About 40 million people live with HIV/AIDS, with ~1.7 million new infections per year[1], and antiretroviral agents (ARVs) targeted towards HIV represent a multi-billion dollar sector to pharmaceutical companies, with continued development of novel agents. Thanks to combination antiretroviral therapy (cART, in which 2 to 4 antiretrovirals [ARVs] are given, simultaneously), individuals infected with HIV (HIV+) during adulthood have a life-expectancy that is nearly normal. HIV+ pregnant women are also maintained on cART till term, and the children are given cART prophylactically at birth. More generally, cART is recommended for all infants and children determined to be HIV+. For all HIV+ patients, if cART is stopped, HIV replication starts up again; thus, HIV+ individuals must remain on cART for the rest of their lives. For HIV+ adults, ARTs are present during aging, a life-stage in which loss of central nervous system (CNS) neurons contributes to loss of cognition and dementia. For HIV+ infants and children, ARTs are also present during a life-stage in which neurodevelopment is occurring and neurodevelopmental disorders manifest (e.g., intellectual disability, autism spectrum disorder, bipolar disorder, schizophrenia).

Approximately 50% of HIV-infected individuals exhibit cognitive impairment[2]. If untreated, HIV-Associated Dementia [HAD], develops, the most severe form of HIV-Associated Cognitive Disfunction (HAND)[3,4]. More mild forms of HAND include asymptomatic neurocognitive impairment (ANI, subjects have impaired cognition, but do not realize it), mild neurocognitive disorder (MND). HIV infects CD4+ peripheral macrophages that migrate to the brain; replication of HIV from these cells may lead to infection of MGs and ACs (but not CNS neurons). As HIV replicates in MG but not in ACs, MG may be a “reservoir” cell type for persistence of HIV infection in the CNS[5]. Mechanisms of neurotoxicity include direct toxic effects of HIV proteins (gp120 and Tat) on neurons, and neuroinflammatory effects in which HIV activates MG and ACs to produce

toxic compounds[6]. HIV may also affect neurogenesis[6], important for both brain development and cognitive function[7,8]. Notably, ANI and MNI persist in HIV+ cART patients, even in cases where viral load is very low. As the HIV+ cART population ages, ANI and MNI might progress to more serious cognitive impairment and the pathways involved are similar to those of Alzheimer's Disease[9,10] (e.g., Aβ-oligomers are elevated[11]). Also, HIV+ children on cART, display reduced IQ and cognition[12-16] and HIV- children, perinatally exposed to cART, experience developmental delays[17]. There is growing concern that cART, itself, may have effects on cognition[18]. For example, cART leads to reduced Myelin Basic Protein in the prefrontal cortex of HAND subjects[19], and HIV+ subjects that withdraw from cART demonstrate improved cognition[20]. EFV (NNRTI) is linked neuropsychiatric effects (e.g., nightmares, dizziness, depression) and cognitive impairment[21-23]. Dolutegravir (DTG) is also linked to neuropsychiatric effects (sleep disturbance, depression)[24-27]. Because of the reservoir of HIV in the CNS, there has been increased effort to improve the penetrance of ARVs into the CNS. A CNS Penetration-Effectiveness (CPE) system ranks ARVs for CNS penetrance, and the higher the CPE scores of the ARVs used in cART, the lower the viral load in the cerebrospinal fluid[28]. While certain studies link cARTs with high CPE to improved neurocognition[29], or no effect[30], others found high CPE correlates with poorer neurocognitive outcome[31,32], including an analysis of 61,938 HIV+ subjects[33]. Brain-penetrant ARVs may immediately reduce HIV and halt cognition defects arising from HIV, itself, but might then later have effects to impair cognition[18]. Physicians must balance the beneficial vs. potentially harmful effects of ARVs[34,35], and a major challenge in drug-discovery is to develop less ARVs that suppress HIV but with less neurotoxicity.

Most in vitro studies have examined potential neurotoxic effects of ARVs on primary embryonic rat cortical neurons. In a seminal study[36] toxic effects on MAP-2 expression (biomarker for neurons) were found for abacavir, EFV, etravirine, nevaripine, and atazanavir, whereas darunavir, FTC, tenofovir, and maraviroc were nontoxic; also, doravirine+abacavir+lamivudine

strongly increased calcium responses to glutamate (potentially increasing excitotoxicity) and didanosine strongly affected mitochondria. Similarly, EFV strongly decreased neuronal viability, reduced neurites and synapses, and reduced excitability of brain slices while tenofovir was less toxic[37]. Akay et al. 2014[38], compared in vivo and in vitro effects of ARVs; in vivo, cART reduced neuronal and synaptic markers in the CNS of SIV-infected monkeys, while cART in uninfected adult rats reduced MAP2 and upregulated proteins associated with anti-oxidation (NQO-1 and HO-1); in vitro (rat neurons), the HIV protease inhibitors ritonavir and saquinovir, alone or in combination, reduced MAP2, increased ROS, and upregulated NQO-1 and HO-1, implicating oxidative effects in the neurotoxicity of ARVs. ARVs also upregulate Beta Secretase 1 (BACE1) which acts on APP to produce Aβ fragments implicated in Alzheimer's pathology, and the Integrated Stress Response (ISR) is involved[39,40]. Also highly relevant, effects of PIs (e.g., lopinavir [LPV]) and INSTIs (e.g., EVG) were compared[41]; EVG was toxic to primary rat neurons (reducing MAP2 by 75%) while LPV reduced MAP2 by 50%.

Virtually all previous in vitro research on the neurotoxicity of HIV ARVs has utilized non-human model systems. The development of human induced pluripotent stem cell technologies, and the ability to differentiate these cells to hiPSC-neurons that represent the brain, provides a new, human in vitro model system for testing HIV ARVs for toxic effects. Notably, automated assay methods have recently been developed, which enable compounds to be tested for toxic or beneficial effects on neurons cultured in 96- or 384-well dishes, to be tested in a high throughput manner; the methods include quantification of neurites and synaptic proteins via immunofluorescence methods, automated digital microscopy, and analysis via image analysis software algorithms (collectively called High Content Analysis (HCA), for the large amount of information that is gathered). Similarly, methods have also been developed for automated analysis of calcium transients (Kinetic Image Cytometry, [KIC]) for neurons cultured in a similar format. In a recent study, for example, tamoxifen, a breast cancer therapeutic agent associated

with post-chemotherapy cognitive impairment, was found to be neurotoxic to primary rat hippocampal neurons, reducing both synaptic puncta and calcium transients as assayed via HCA and KIC methods[42]. The goal of the present study was to test certain HIV-ARVs for neurotoxicity on hiPSC-neurons and use HCA and KIC methods to quantify effects on neuronal structures and biomarkers, and neuronal function.

A second goal was to test HIV ARVs for effects relevant to neurogenesis, a process via which neural precursor cells (NPCs) differentiate to neurons, both in the embryonic brain, and, also, adult brain. Notably, zidovidine (AZT) and tenofovir disoproxil fumarate (TDF) reduce the viability of murine NPCs[43,44] but, to our knowledge, there are no reports in which HIV ARVs have been tested on human NPCs. Additionally, as regulation of differentiation is often associated with altered epigenetic control of chromatin structure, we quantified effects of HIV ARVs in the human NPCs via the recently developed Microscopic Imaging of Epigenetic Landscapes (MIEL) assay, which uses a multiparametric approach to identify subtle changes in the patterns of histone acetylation and methylation, as imaged via immunofluorescence, and assayed via HCA.

Our main finds were that EVG had a strong effect, strongly reducing neurites, synaptic puncta, and calcium activity of hiPSC-glutamatergic neurons, when tested alone, or in combination with TDF and FTC. Milder, but significant, effects were also obtained with DTG and TDF on neuronal viability, neurites, and synapses. Regarding neurogenesis and epigenetic effects, TDF reduced viability of the human NPCs, and had a significant effect to alter the epigenetic, histone acetylation/methylation, as assayed via the MIEL assay.

Materials and Methods

Cell Culture. For hiPSC-glutamatergic neuron experiments, imaging-quality polystyrene 384-well plates (Greiner Bio-One #781090; Frickenhausen, Germany) were coated with 0.1% polyethyleneimine and 0.028 mg/mL growth factor-reduced Matrigel (Corning Life Sciences #354230, Tewksbury, MA, USA). iPSC-derived glutamatergic neurons (iCell GlutaNeurons; Fujifilm CDI #C1060, Madison, WI, USA) were seeded at a density of 60,000 live cells/cm^2 and were maintained per the manufacturer's instructions for a total of 14 days before assay.

For fetal neural precursor cell (hNPC) experiments, imaging-quality polystyrene 384-well plates (Greiner Bio-One #781090; Frickenhausen, Germany) were coated with 0.028 mg/mL growth factor-reduced Matrigel (Corning Life Sciences #354230, Tewksbury, MA, USA). hNPCs (ThermoFisher # A15654) were seeded at a density of 18,200 live cells/cm^2 and were maintained in differentiation medium per the manufacturer's instructions for a total of 7 days before assay (ARVs were added for the final 3 days).

Test Compounds. Glutamatergic neuron cultures were treated with ARVs and ARV combinations for 1 or 7 days prior to assays. The following ARVs and combinations were used in this study: dolutegravir (DTG; Toronto Research Chemicals #D528800; Toronto, ON, Canada), elvitegravir (EVG; Toronto Research Chemicals #E509000), tenofovir disaproxil fumarate (TDF; Toronto Research Chemicals #T018505), emtricitabine (FTC; Toronto Research Chemicals #E525000), DTG+TDF+FTC, EVG+TDF+FTC, and TDF+FTC. Vehicle (0.2% DMSO) and antagonist control treatments (25 µM *para*-nitroblebbistatin; Optopharma Ltd. #DR-N-111; Budapest, Hungary) were also applied to the cells in addition to the ARVs/ARV combinations. Fetal neural precursor cells were treated with 0.2% DMSO, ARVs, SAHA (Cayman Chemical #10009929), GSK343 (Cayman

Chemical #14094), Tofacitinib (TOF, Cayman Chemical #11598), or (+)-JQ1 (Cayman Chemical #11187).

Automated Microscopy. Both the fixed-endpoint synaptic density and neurite outgrowth assay and the live-cell calcium kinetic image cytometry (KIC®) assay were imaged using the IC200-KIC® automated microscope (Vala Sciences Inc.; San Diego, CA, USA) outfitted with a Plan Apo 20X/0.75 NA objective lens (Nikon Instruments Inc.; Melville, NY, USA). For live-cell assays, the environmental chamber of the IC200-KIC® was set to 37°C/5% CO_2.

Synaptic Density and Neurite Outgrowth Assay. After treatment, cells were fixed in 2% paraformaldehyde/1.67% sucrose in HBSS without Ca^{++}/Mg^{++}, permeabilized in 0.3% Triton X-100 in PBS with Ca^{++}/Mg^{++}, and blocked in 5% normal goat serum/1% BSA/0.1% Triton X-100. The following primary antibodies were diluted in blocking buffer and applied to cells overnight at 4°C: chicken anti-βIII tubulin (1:200; Abcam #ab41489; Boston, MA, USA), rabbit anti-PSD95 (1:200; Thermo Fisher Scientific #51-6900; Waltham, MA, USA), and mouse anti-SV2 (1:150; Developmental Studies Hybridoma Bank; Iowa City, IA, USA). The next day, the following secondary antibody cocktail with Hoechst nuclear stain was made in 2% BSA and applied to the cells for 1 hr at room temperature in the dark: goat anti-chicken IgY Alexa Fluor 555 (1:500; Thermo Fisher Scientific #A21437), goat anti-rabbit IgG Alexa Fluor 647 (1:500; Thermo Fisher Scientific #A21245), goat anti-mouse IgG Alexa Fluor 488 (1:500; Thermo Fisher Scientific #A11029), and 10 µg/mL Hoechst 33342 (Thermo Fisher Scientific #H3570). For each well, a 3 FOV-by-3 FOV matrix of images was acquired in each optical channel.

Calcium KIC® Assay. Neurons were loaded with a calcium indicator dye solution consisting of 5 µM Rhod-4 AM (AAT Bioquest #21122; Sunnyvale, CA, USA), 1X PowerLoad (Thermo Fisher Scientific #P10020), 1 µg/mL Hoechst 33342, and 2.5 mM probenecid in phenol red-free BrainPhys (Stemcell Technologies #05791; Vancouver, BC, Canada) for 40 min at 37°C. The

neurons were then rinsed with and imaged under phenol red-free BrainPhys. One FOV was imaged per well; calcium movies were acquired at 4 fps for 2 min.

hNPC Microscopic Imaging of Epigenetic Landscape (MIEL) Assay. After treatment, cells were fixed in 2% paraformaldehyde/1.67% sucrose in HBSS without Ca^{++}/Mg^{++} and blocked/permeabilized in PBS with Ca^{++}/Mg^{++} and 2% BSA/0.5% Triton X-100. The following primary antibodies were diluted in blocking buffer and applied to cells overnight at 4°C: rabbit H3K9me3 (1:500; Active Motif, 39765); mouse H3K4me1 (1:100; Active Motif, 39635); mouse H3K27me3 (1:250; Active Motif, 61017); rabbit H3K27ac (1:500; Active Motif, 39133); and chicken NeuN (1:100; Abcam, ab134014). The next day, the following secondary antibody cocktail with Hoechst nuclear stain was made in 2% BSA and applied to the cells for 1 hr at room temperature in the dark: goat anti-chicken IgY Alexa Fluor 555 (1:500; Thermo Fisher Scientific #A21437), goat anti-rabbit IgG Alexa Fluor 647 (1:500; Thermo Fisher Scientific #A21245), goat anti-mouse IgG Alexa Fluor 488 (1:500; Thermo Fisher Scientific #A11029), and 10 µg/mL Hoechst 33342 (Thermo Fisher Scientific #H3570).

Automated Image Analysis. For hiPSC-Glut synapse density, neurite outgrowth, and calcium KIC® assays, images were analyzed using custom algorithms in CyteSeer® software (Vala Sciences Inc.). For the hNPC MIEL assay, images were analyzed using Acapella 2.6 (PerkinElmer), and image features were analyzed as described in Farhy, et al., eLife, 2019, DOI: 10.7554/eLife.49683.

Statistical Analysis. The data were analyzed with Prism (GraphPad Software; San Diego, CA, USA) using ANOVA, followed by Dunnett's post-hoc multiple comparisons test for statistical significance (*p<0.05, **p<0.01, ***p<0.001).

Results:

Effects of HIV ARVs on neuronal biomarkers and structures (neuronal viability, neurites, and synapses, assayed via HCA): In an initial experiment, we exposed hiPSC-glutamatergic neurons seeded on a 384 well plates, were exposed to 0.1, 1.0, and 10 μM DTG, EVG, TDF, FTC, for 7 days. Blebbistatin, at 25 μM, an inhibitor of non-muscle myosin, was also included as a control compound. The cells were then fixed and immunolabeled for Tuj-1 (neuronal marker), SV2 (a presynaptic protein), and PSD95 (post-synaptic protein), stained for nuclei (with Hoeschst), and imaged with the IC200 Image Cytometer (9 fields of view (FOV) per well, in a 3 x 3 matrix, with images in 4 fluorescence channels). While the 1 day exposure generally had little, or very mild effects (data not shown), 7 day exposure to the HIV ARVs led to neurotoxic effects on the hiPSC-gluts, with DTG, EVG, TDF, each tested at 10 μM, reducing and altering neurite morphology (Fig. 1A displays representative images, with EVG having the strongest effect). A nuclear recognition algorithm within CyteSeer® was used to quantify the effects of ARVs on Neuronal Viability (nuclei associated with Tuj-1 staining in the cell bodies) and this was reduced by about 25%, 65%, and 30% by 10 μM DTG, 10 μM EFG, and 10 μM TDF, respectively (Fig. 1B). An algorithm within CyteSeer® also recognized and segmented the Tuj-1 label, and tabulated the length of the identified neurites per area to yield Total Neurite Length; this was mildly affected mildly affected DTG (~20% reduction) and 10 μM TDF (~30% reduction) and strongly affected by 10 μM EVG (80% reduction) (Fig. 1C). We also calculated the Neurite Length per Neuron (dividing Total Neurite Length by the Neuronal Nuclei); for this parameter, 10 μM DTG led to a mild (about 20%, $p<005$) increase, whereas 10 μM EVG strongly diminished this value by (50%, $p<0.001$, Fig. 1D). Blebbistatin also had a slight inhibitory effect on this parameter (~10 % reduction, $p < 0.05$). Notably, FTC had no effect on these parameters, for any of the concentrations tested.

In a second set of experiments, hiPSC-gluts were exposed to HIV ARVs at 10 μM, alone (DTG, EVG, TDF, and FTC) or in combination (DTG/TDG/FTC, EVG/TDF/FTC, or TDF/FTC) for 1 or 7 days. For hiPSC-Gluts tested for 1 day, the combination of DTG/TDF/FTC had a mild (10% reduction) effect on Neuronal Viability (Fig. 2A), whereas the other treatments were without effect, Neurite Length (Fig. 2B) was unaffected by the ARVs, but mildly increased (about 15%) by blebbistatin, and Neurite Length per Neuron (Fig. 2C) was not altered by any treatment. In contrast, exposure to the ARVs for 7 days had notable neurotoxic effects. Neuronal Viability (Fig. 2D) was mildly reduced by DTG (~25 %), strongly reduced by EVG (80%), moderately reduced by TDF (~30%) strongly reduced by DGT/TDF/FTC (~75%), strongly reduced by EVG/TDF/FTC (~85%) and moderately reduced by TDF/FTC (~35%). Neurite Length (Fig 2E) was slightly reduced by DTG (~15%), strongly reduced by EVG (85%), strongly reduced by DTG/TDF/FTC (70%) and very strongly reduced by EVG/TDF/FTC (~90%), and slightly increased (~15%) by blebbistatin. The parameter Neurite Length per Neuron (Fig. 2F) was not significantly changed by any treatement, though there was increased variability for the data for EVG, and the combinations DTG/TDF/FTC and EVG/TDF/FTC. Overall, it is worth noting that FTC, again was nontoxic to the hiPSC-Gluts. Also, there was good agreement between the inhibitory effects of DTG, EVG, and TDF, in this experiment (all tested at 10 μM) with the data obtained for these agents at 10 μM in the previous experiment. Regarding combinations of ARVs, the inhibitory effects of EVG/TDF/FTC were similar to the effect of EVG, by itself, on Neuronal Viability and Neurite Length, suggesting that the EVG was the dominant neurotoxic component for the mixture. In contrast, the combination of DTG/TDF/FTC appeared to be more toxic than either DTG or TDF, suggesting a potential additive effect of these agents.

Next, we quantified synaptic puncta, utilizing algorithms within CyteSeer® that identify SV2 puncta and PSD95 puncta in close proximity to each other, and also along the Tuj1 positive neurites from the two different experiments. Representative images from hiPSC-Gluts treated for

7 days with ARVs are shown in Figure 3A labeled for SV2, PSD95, and also a separate series of images depicting the "masks" identified by CyteSeer® to represent nuclei, neurites, and synapses. Synapse Count (Figure 3B), which is the count of synaptic puncta by area, was significantly reduced by 1 μM DTG (~30%, $p < 0.001$), 0.1 μM EVT (25%),strongly by 10 μM EVT (~80%), moderately by TDF at 1 μM (~30%) and 10 μM (~40%), and moderately by FTC at 1 μM (~25%) and 10 μM (30%), and moderately by blebbistatin (~28%). Synapse/Neurite Length (Figure 3C), which is the Synapse Count normalized to combined length of the neurites was altered in a complex manner by the ARVs. For example, this parameter was decreased mildly by 0.1 μM DTG (~15%) and moderately by 1 μM DTG (~33%) but the value for 10 μM 10 DTG was virtually equivalent to DMSO. EVG decreased this parameter at 0.1 μM (~30%), had no significant effect at 1 μM, and increased this value (~15%) at 10 μM. TDF diminished this parameter, moderately at all doses (25%, 30%, and 25% for 0.1, 1, and 10 μM). And, interestingly, FTC also inhibited this parameter at all doses (25%, 33%, and 25%, for 0.1, 1, and 10 μM, respectively). Blebbistatin also reduced this parameter (25%). Overall, the effects of the ARVs on the Synapse Count are similar to the data from this experiment for neuronal viability and neurite length (e.g., Fig. 1).

Regarding quantification of synapses from the experiment in which the ARVs were tested alone, and in combination at 10 μM, after 1 day of treatment none of the ARVs had an effect on Synapse Count (Figure 4A), and this parameter was mildly increased (~15%) by blebbistatin, and none of the treatments altered Synapses/Neurite Length (Figure 4B). In contrast, treatment for 7 days, led to strong reduction in Synapse Count (Figure 4C) by EVG (~85%) a moderate reduction by DTG/TDF/FTC (~65%) and a mild reduction by TDF/FTC (~20%). Regarding Synapses/Neurite Length, the only condition that had an effect was TDF/FTC which caused a mild reduction (~25%).

Effects of HIV ARVs on neuronal calcium (calcium transients assayed via KIC): In another set of experiments, hiPSC-Gluts seeded in 384-well dishes were exposed to the ARVs alone, or in combination, at 10 μM each for 1 or 7 days, then loaded with Hoechst and the calcium indicator Rhod-4. To perform KIC imaging and analysis, plates were placed into the IC200-KIC which navigated to each well and collected a single image in the nuclear channel; the instrument then switched to the Rhod-4 channel and collected a digital movie at 4 fps for 2 minutes. After imaging, algorithms within CyteSeer® compared the nuclear image to the movie of Rhod-4 fluorescence and identified the cell bodies associated with each neuron in the field of view. The average pixel intensity (API) for each cell body was then calculated for every frame of the movie, to enable quantification of the calcium transients that occurred in each cell during the recording period. In addition to identifying and counting each transient, additional parameters were also calculated including transient magnitude, duration, and upstroke and down stroke kinetics, an approach originally developed for quantifying calcium transients in cardiac myocytes[45].

Representative calcium transients are shown for the hiPSC-Gluts exposed to either DMSO or the ARVs for 7 days in Figure 5. hiPSC-Gluts exposed to DMSO for 7 days typically display several calcium transients per cell, over the 2- minute recording period, with durations lasting 2 to 60 sec (Figure 5A). In contrast, DTG had a moderate effect to reduce activity (Figure 5B), EVG strongly reduced activity (Figure FC), whereas TDF (Figure FD) and FTC (Figure FE) had more milder effects. The combination of DTG/TDF/FTC reduced activity (Figure 5F) and this effect appears to be stronger the effect of DTG by itself. The combination of EVG/TDF/FTC very strongly reduced activity (Figure 5G), whereas neurons exposed to TDF/FTC (Figure 5H) displayed activity that was nearly the same as those exposed to DMSO.

The quantification of calcium transient activity for cells exposed to ARVs for 1 or 7 days is shown in Figure 6. For cells exposed to ARVs for 1 day, no significant effects were observed on the Percent Active parameter (the number of active neurons divided by the total number of

neurons in the field of view), the Event Frequency (calcium transients per second), or the Mean Peak Amplitude (the average magnitude of the transients for each neuron, averaged across each active neuron in the field of view). In contrast, exposure to ARVs for 7 days had marked, inhibitory, effects on calcium activity. For example, the Percent Active parameter (Figure 6D) was moderately reduced by DTG(~30%), strongly reduced by EVG (~85%), strongly reduced by DTG/'TDF/FTC (70%), very strongly reduced by EVG/TDF/FTC (~90%) and moderately reduced by TDF/FTC (~25%). The Even Frequency parameter (Figure 6E) was moderately reduced by EVG (~40%), moderately reduced by DTG/TDF/FTC (~30%), and strongly reduced by EVG/TDF/FTC (~65%). The Mean Peak Amplitude parameter (Figure 6F) was strongly reduced by EVG (~65%), and by EVG/TDF/FTC (~63%). Notably, TDF and FTC, by themselves appeared to have no effect on the Percent Active, Event Frequency, or Mean Peak Amplitude parameters.

Effects of ARVs on hNPCs (cell viability and MIEL analysis): Viability of the hNPCs was not affected by a 3 day exposure to 0.1 μM, 1 μM, or 10 μM DTG, EVG, or FTC. However, TDF, at 10 μM, significantly reduced viability (~28%) (Figure 7A). Viability of the hNPCs was also reduced more strongly by 3 μM SAHA (~45%), a histone deacetylase inhibitor, and by 10 μM GSK343 (~53%), an inhibitor of the histone methyltransferase, EZH2. Viability of the hNPCs was not affected by 0.3 μM JQ1, which inhibits the interaction of proteins with acetylated histones, or tofacitinib (TOF), an inhibitor of JAKi.

For the MIEL analysis, immunolabeling was done in two sets: cells in one 384 well plate were simultaneously labeled for H3K9me3 (condensed chromatin) and H3K4me1 (active promoters), whereas cells in a sister dish (same plate map) were labeled for H3K27me3 (associated with condensed chromatin) and H3K27ac (active promoters). The plates were then scanned using Vala's IC200 image cytometer, and the images for each channel were analyzed via digital image analysis algorithms that first identify the nuclei of each cell; the patterns of marks within each nucleus are then analyzed creating multivariate signatures or "finger-prints" of each

perturbation. Texture features[46-48] are used rather than intensities and morphologies, thus reducing culturing and immunolabeling artifacts. The results from discriminant analysis, plotted in 2D, are shown in this report to illustrate shifts in the epigenetic signatures in response to test compounds. For each plate (H3K27me3/H3K27ac, Figure 7B, and HeK9me3/H3K4me1, Figure 7C). GSK343 had strong effects on MIEL signature, with data points representing each well treated with GSK343 clustering by themselves, far removed from samples treated with DMSO or the ARVs. SAHA also had strong effects on the MIEL signature, with data points from this compound clustering together, far removed from samples treated with DMSO or the ARVs, and also well removed from the GSK343 samples. The samples for SAHA were displaced from DMSO in a different direction in the display, compared to GSK343, which is expected since SAHA and GSK343 affect different epigenetic pathways. Interestingly, of the ARVs, only TDF at the highest concentration (10 μM), altered the MIEL signature; the data points for 10 μM TDF cluster, by themselves, in both the H3K27me3/H3K27ac and H3K9me3/H3K4me1 plots (Figure 7B and 7C). The results for TDF also are closer to the data for GSK343 compared to SAHA in both plots. For strategies such as this, in which multiparametric analyses approaches are used to stratify responses to compounds in multi-dimensional space, it is useful to mathematically test the accuracy via which the algorithms can successfully recognize whether or not a sample falls into the cluster group that has been identified for a particular treatment. This is done in the mathematical modeling, and the results presented in the form of a “Confusion Matrix”. In the Confusion Matrix for the H3K27me3/H3K27ac comparison (Figure 7D), for example, wells exposed to GSK343 at 10 μM were recognized by the algorithm as belonging to the GSK343 cluster, 100% of the time. Similarly, 100% recognition occurred for wells treated with SAHA, and, importantly, for 10 μM TDF. In contrast, wells treated with DMSO were classified by the algorithm correctly into the DMSO cluster, only 33% of the time; this low value is because the wells for DTG, EVG, FTC, JQ1, and TOF all clustered with DMSO (so wells in this area of the plot can not be accurately assigned to DMSO, or the other ARVs). The confusion matrix for the

H3K9me3/H3K4me1 comparison also demonstrates 100% recognition by the algorithm of wells for GSK343, for SAHA, and 10 μM TDF.

Overall, the results suggest that TDF can reduce viability and alter the patterns of epigenetic histone tags within the nuclei of hNPCs.

Discussion

In this study, HCA and KIC methods developed to quantify neurotoxic effects of tamoxifen in primary rat hippocampal neurons[42] were adapted to identify and quantify potential neurotoxic effects of HIV ARVs in hiPSC-Gluts, which are representative of human excitatory cortical neurons, a cell type whose survival is important for cognitive function. Thus, loss of excitatory neurons, in response to ARVs could conceivably contribute to HAND, which afflicts a large percentage of the current HIV+ population, and which is very likely to increase in incidence and severity as the HIV+ population ages. While neurotoxicity of ARVs has been suspected for certain HIV ARVs, for some time (as certain ARVs have been linked to psychological and cognitive effects), and, indeed, pathologies reminiscent of Alzheimer's have been observed, post-mortem, brain sections for HIV+ patients on cART. Also, fetuses of pregnant HIV+ women are often exposed to cART from conception, and cART is given perinatally (before birth, and soon after birth) to children born to HIV+ women, routinely, to prevent mother-to-child transmission. Furthermore, children of any age can be infected by HIV+ (via breast milk, for example), and are also then prescribed cART. While it is necessary to prescribes ARVs and cART to prevent HIV replication (and subsequent development of AIDS), many studies have revealed developmental delays in children on cART, including those in which the exposure was just perinatal[49]. Thus, there is a strong need for in vitro systems, utilizing human neurons and neuronal precursors to test HIV ARVs for neurotoxic/neurodevelopmental effects. The strategies used in this study feature automated digital microscopy and analysis for cells plated in 384-well dishes, a format that leads to higher throughput testing of ARVs; thus, a many ARVs can be tested in parallel, dose-response relationships can be tested, and ARVs can be tested in combination corresponding to different cART regimes.

Previous studies of the neurotoxicity of ARVs in vitro, have largely been conducted with primary embryonic rat neurons. Interestingly, exposure of these cells to 10 μM EVG for 4 days

led to a substantial reduction in MAP2+ neurons in the culture[41]. In our hands, EVG was also toxic to hiPSC-Gluts, confirming the neurotoxicity of this compound in a human neuron model. We also observed more mild toxic effects of DTG, a first-line integrase strand inhibitor, and the nucleoside/nucleotide reverse transcriptase inhibitor, TDF on the hiPSC-Gluts. These agents are very widely prescribed, and in general are largely considered safe. Our data, however, suggests that therapeutic window for use of these ARVs may be narrower than is commonly suspected, which is concerning. Overall, FTC was relatively non-toxic in our hands.

Very recently, a model has been developed, which enables the testing of ARVs on cocultured hiPSC-neurons/-microglia/-astrocytes, which is very important since ARVs could elicit neurotoxicity, indirectly, by activating microglia and astrocytes to release neuroinflammatory compounds, and, indeed, efavirenz (EFZ), a NNRT linked to neuropsychiatric/cognitive effects, elicited release of TNF-alpha from the hiPSC-microglia in the system[50]. The system also enables testing of the efficacy of ARVs to inhibit HIV infection of human microglia, which will be important in future studies, where there will be a clear goal to increase ARV efficacy in this cell type, with minimal neurotoxicity. This system also represents a likely candidate for the automated imaging and analysis methods of the present study.

Our results also indicate that TDF reduces that viability of hNPCs. TDF reduces viability of murine NPCs, in vitro[43], and our results confirm this toxicity for human NPCs. Given the importance of neurogenesis in both embryonic development and maintenance of cognitive function (reduced neurogenesis in the adult hippocampus, for example, occurs in Alzheimer's Disease), it is critically important to evaluate existing and candidate ARVs for such effects on human NPCs. TDF also altered the distribution pattern of histone tags in hNPCs, which is interesting, as such shifts are often associated with effects on differentiation. Notably, DNA-methylation, another epigenetically regulated parameter, has recently been reported to be altered in HIV+children receiving cART[51].

In summary, we have developed and applied methods for the high throughput testing of HIV ARVs on hiPSC-Gluts, which represent excitatory neurons of the human brain, and also test methods to assess the effects of HIV ARVs on the viability and epigenetic properties of human neural precursor cells. It would be beneficial to society to develop HIV ARVs that are efficacious in suppressing HIV replication with minimal neurotoxicity/neurodevelopmental effects. The results of the present study represent progress in this direction. Future directions will include incorporation of human neuroimmune cells (hiPSC-microglia and hiPSC-astrocytes), into the system to increase the relevance of the test system to identifying neurotoxic and neurodevelopmental effects of existing and candidate anti-HIV therapeutics.

Acknowledgements:

This study was funded, in part, by grants from the NIH, which include R44ES026268 “Assay of chemicals for Parkinson's toxicity in human iPSC-derived neurons” and R41MH119621 “The Microscopic Imaging of Epigenetic Landscape- NeuroDevelopment (MIEL-ND) assay”

Figure Legends

Figure 1. ARVs decrease viability and neurite length in hiPSC-Gluts. (A) Representative images of hiPSC-Gluts treated with DMSO alone or 10 μM dolutegravir (DTG), elvitegravir (EVG), tenofovir disproxil fumarate (TDF), or emtricitabine (FTC), fixed, and stained for nuclei (Hoechst, blue) and neuronal somas and neurites (Tuj-1, grayscale). Scale bar = 50 μm. (B-D) Viability and neurite data for hiPSC-Gluts treated with DMSO alone, ARVs (0.1, 1, or 10 μM) or blebbistatin (25 μM). (B) Neuronal viability as defined by the number of live neuron nuclei in each well relative to the DMSO control mean. (C) Total neurite length in μm per cm^2 image area for each condition. (D) Total neurite length per live neuron nucleus for each condition. Each dot represents the average of each measurement from nine images per well. DMSO and blebbistatin: n = 18 wells; ARVs: n = 6 wells. Bars represent mean ± standard deviation. Statistics performed with one-way ANOVA followed by Dunnett's multiple comparisons test. * $p < 0.05$, ** $p < 0.01$, *** $p < 0.001$.

Figure 2. ARVs decrease viability and neurite length in hiPSC-Gluts after seven days, but not one day of exposure. hiPSC-Gluts were treated for one (left) or seven days (right) with DMSO alone, 25 μM blebbistatin, single ARVs, or combinations of ARVs (each at 10 μM). (A, D) Neuronal viability as defined by the number of live neuron nuclei in each well relative to the DMSO control mean. (B, E) Total neurite length in μm per cm^2 image area in each well relative to the DMSO control mean. (C, F) Total neurite length per live neuron nucleus in each well relative to the DMSO control mean. Each dot represents the average of each measurement from nine images per well. One-day treatment DMSO and blebbistatin: n = 18 wells; ARVs: n = 6 wells. Seven-day treatment DMSO and blebbistatin: n = 36 wells; ARVs: n = 12 wells from two

experiments. Bars represent mean ± standard deviation. Statistics performed with one-way ANOVA followed by Dunnett's multiple comparisons test. * $p < 0.05$, ** $p < 0.01$, *** $p < 0.001$.

Figure 3. ARVs affect synapse count and density in hiPSC-Gluts. (A) Representative images of hiPSC-Gluts from the same experiment in Figure 1 stained for SV2 (presynaptic marker, left) and PSD95 (postsynaptic marker, right). Right images show live neuron nuclei (green), neurites (cyan), and synapses (magenta) identified by CyteSeer®. Scale bar = 50 µm. (B) Synapse count per μm^2 for each condition. (C) Synapse count per µm neurite length for each condition. Each dot represents the average of each measurement from nine images per well. DMSO and blebbistatin: n = 18 wells; ARVs: n = 6 wells. Bars represent mean ± standard deviation. Statistics performed with one-way ANOVA followed by Dunnett's multiple comparisons test. * $p < 0.05$, ** $p < 0.01$, *** $p < 0.001$.

Figure 4. ARVs affect synapse count and density if hiPSC-Gluts after seven days, but not one day of exposure. hiPSC-Gluts were treated for one or seven days with DMSO alone, 25 µM blebbistatin, single ARVs, or combinations of ARVs (each at 10 µM). (A, C) Synapse count per μm^2 in each well relative to the DMSO control mean. (B, D) Synapse count per µm neurite length in each well relative to the DMSO control mean. Each dot represents the average of each measurement from nine images per well. One day treatment DMSO and blebbistatin: n = 18 wells; ARVs: n = 6 wells. Seven day treatment DMSO and blebbistatin: n = 36 wells; ARVs: n = 12 wells from two experiments. Bars represent mean ± standard deviation. Statistics performed with one-way ANOVA followed by Dunnett's multiple comparisons test. * $p < 0.05$, ** $p < 0.01$, *** $p < 0.001$.

Figure 5. Effect of ARVs on calcium transients in hiPSC-Gluts. hiPSC-Gluts were treated for seven days with DMSO alone, single ARVs, or combinations of ARVs (each at 10 μM). (A-H) Traces shown for active neurons in each well and base line is subtracted to display the calcium transient activity for each cell. DMSO: 1034 cells; DTG: 716 cells; EVG: 31 cells; TDF: 729 cells; FTC: 1003 cells; DTG/TDF/FTC: 134 cells; EVG/TDF/FTC: 17 cells; TDF/FTC: 539 cells. Six wells per condition.

Figure 6. Quantification of the effects of ARVs on calcium activity in hiPSC-Gluts. hiPSC-Gluts were treated for one or seven days with DMSO alone, single ARVs, or combinations of ARVs (each at 10 μM). (A, D) Percent of live neurons that are active with detectable calcium transients in each condition. (B, E) The mean event frequency of calcium transients of all active neurons in each well. (C, F) The mean of mean calcium peak amplitudes of all active neurons in each well. Six wells per condition. Bars represent mean ± standard deviation. Statistics performed with one-way ANOVA followed by Dunnett's multiple comparisons test. * $p < 0.05$, ** $p < 0.01$, *** $p < 0.001$.

Figure 7. Tenofovir disproxil fumarate affects the viability and epigenetic signature of hNPCs. Fetal hNPCs were treated with DMSO alone, compounds with known epigenetic effects (SAHA, GSK343, JQ1, or TOF), or ARVs at the indicated concentrations. (A) Count of hNPCs per well for each condition following treatment. Bars represent mean ± standard deviation. Statistics performed with one-way ANOVA followed by Dunnett's multiple comparisons test. * $p < 0.05$. (B-E) Quadratic discriminant analysis using texture features derived from images of hNPCs treated with the indicated compounds and immunostained for H3K27me3 and H3K27ac (B, D) or H3K9me3 and H3K4me1 (C, E). (B, C) Scatter plots showing the first two texture-derived

discriminant factors for each condition. (D, E) Confusion matrices showing the results of the discriminant analysis. Numbers represent the percent of wells classified correctly (on the diagonal) and incorrectly (off the diagonal). N = 6 wells per condition.

References

1. Anonymous. Global HIV & AIDS statistics — 2020 fact sheet. Vol. 2020 (UNAIDS, 2020).
2. Smail, R.C. & Brew, B.J. HIV-associated neurocognitive disorder. *Handbook of clinical neurology* **152**, 75-97 (2018).
3. Navia, B.A., Cho, E.S., Petito, C.K. & Price, R.W. The AIDS dementia complex: II. Neuropathology. *Ann Neurol* **19**, 525-535 (1986).
4. Navia, B.A., Jordan, B.D. & Price, R.W. The AIDS dementia complex: I. Clinical features. *Ann Neurol* **19**, 517-524 (1986).
5. Wallet, C.*, et al.* Microglial Cells: The Main HIV-1 Reservoir in the Brain. *Frontiers in cellular and infection microbiology* **9**, 362 (2019). PMCID PMC6821723.
6. Kaul, M. HIV's double strike at the brain. *Front Biosci.* **13**, 2484-2494 (2012).
7. Hollands, C., Bartolotti, N. & Lazarov, O. Alzheimer's Disease and Hippocampal Adult Neurogenesis; Exploring Shared Mechanisms. *Frontiers in neuroscience* **10**, 178 (2016). PMCID PMC4853383.
8. Urban, N. & Guillemot, F. Neurogenesis in the embryonic and adult brain: same regulators, different roles. *Frontiers in cellular neuroscience* **8**, 396 (2014). PMCID PMC4245909.
9. Milanini, B. & Valcour, V. Differentiating HIV-Associated Neurocognitive Disorders From Alzheimer's Disease: an Emerging Issue in Geriatric NeuroHIV. *Current HIV/AIDS reports* **14**, 123-132 (2017). PMCID PMC5823609.
10. Canet, G.*, et al.* HIV Neuroinfection and Alzheimer's Disease: Similarities and Potential Links? *Frontiers in cellular neuroscience* **12**, 307 (2018). PMCID PMC6141679.
11. Stern, A.L.*, et al.* BACE1 Mediates HIV-Associated and Excitotoxic Neuronal Damage Through an APP-Dependent Mechanism. *J Neurosci* **38**, 4288-4300 (2018). PMCID PMC5932640.
12. Cohen, S.*, et al.* Poorer cognitive performance in perinatally HIV-infected children versus healthy socioeconomically matched controls. *Clin Infect Dis* **60**, 1111-1119 (2015).
13. Van den Hof, M.*, et al.* Lower IQ and poorer cognitive profiles in treated perinatally HIV-infected children is irrespective of having a background of international adoption. *PLoS One* **14**, e0224930 (2019). PMCID PMC6894817.
14. Sherr, L., Croome, N., Castaneda, K. P., Bradshaw, K., Romero, R. H. Developmental challenges in HIV infected children - An updated systemic review. *Children and Youth Services Review* **45**, 74-89 (2014).
15. Sherr, L., Croome, N., Bradshaw, K. & Parra Castaneda, K. A systematic review examining whether interventions are effective in reducing cognitive delay in children infected and affected with HIV. *AIDS Care* **26 Suppl 1**, S70-77 (2014).
16. Crowell, C.S., Malee, K.M., Yogev, R. & Muller, W.J. Neurologic disease in HIV-infected children and the impact of combination antiretroviral therapy. *Rev Med Virol* **24**, 316-331 (2014).
17. Sherr, L., Croome, N., Parra Castaneda, K. & Bradshaw, K. A systematic review of psychological functioning of children exposed to HIV: using evidence to plan for tomorrow's HIV needs. *AIDS Behav* **18**, 2059-2074 (2014).
18. Underwood, J., Robertson, K.R. & Winston, A. Could antiretroviral neurotoxicity play a role in the pathogenesis of cognitive impairment in treated HIV disease? *AIDS* **29**, 253-261 (2015).
19. Jensen, B.K.*, et al.* Altered Oligodendrocyte Maturation and Myelin Maintenance: The Role of Antiretrovirals in HIV-Associated Neurocognitive Disorders. *Journal of neuropathology and experimental neurology* **74**, 1093-1118 (2015). PMCID PMC4608376.

20. Robertson, K.R., *et al.* Neurocognitive effects of treatment interruption in stable HIV-positive patients in an observational cohort. *Neurology* **74**, 1260-1266 (2010). PMCID PMC2860482.
21. Apostolova, N., *et al.* Efavirenz and the CNS: what we already know and questions that need to be answered. *J Antimicrob Chemother* **70**, 2693-2708 (2015).
22. Hakkers, C.S., *et al.* Objective and Subjective Improvement of Cognition After Discontinuing Efavirenz in Asymptomatic Patients: A Randomized Controlled Trial. *J Acquir Immune Defic Syndr* **80**, e14-e22 (2019).
23. Lapadula, G., *et al.* Switching from efavirenz to rilpivirine improves sleep quality and self-perceived cognition but has no impact on neurocognitive performances. *AIDS* **34**, 53-61 (2020).
24. Chan, P., *et al.* Neuropsychiatric outcomes before and after switching to dolutegravir-based therapy in an acute HIV cohort. *AIDS Res Ther* **17**, 1 (2020). PMCID PMC6945418.
25. Elliot, E.R., *et al.* Increased Dolutegravir Peak Concentrations in People Living With Human Immunodeficiency Virus Aged 60 and Over, and Analysis of Sleep Quality and Cognition. *Clin Infect Dis* **68**, 87-95 (2019).
26. Hoffmann, C. & Llibre, J.M. Neuropsychiatric Adverse Events with Dolutegravir and Other Integrase Strand Transfer Inhibitors. *AIDS Rev* **21**, 4-10 (2019).
27. de Boer, M.G., *et al.* Intolerance of dolutegravir-containing combination antiretroviral therapy regimens in real-life clinical practice. *AIDS* **30**, 2831-2834 (2016).
28. Letendre, S., *et al.* Validation of the CNS Penetration-Effectiveness rank for quantifying antiretroviral penetration into the central nervous system. *Arch Neurol* **65**, 65-70 (2008). PMCID PMC2763187.
29. Tozzi, V., *et al.* Changes in cognition during antiretroviral therapy: comparison of 2 different ranking systems to measure antiretroviral drug efficacy on HIV-associated neurocognitive disorders. *J Acquir Immune Defic Syndr* **52**, 56-63 (2009).
30. Santos, G.M.A., *et al.* Cross-Sectional and Cumulative Longitudinal Central Nervous System Penetration Effectiveness Scores Are Not Associated With Neurocognitive Impairment in a Well Treated Aging Human Immunodeficiency Virus-Positive Population in Switzerland. *Open Forum Infect Dis* **6**, ofz277 (2019). PMCID PMC6612860.
31. Marra, C.M., *et al.* Impact of combination antiretroviral therapy on cerebrospinal fluid HIV RNA and neurocognitive performance. *AIDS* **23**, 1359-1366 (2009). PMCID PMC2706549.
32. Kahouadji, Y., *et al.* Cognitive function after several years of antiretroviral therapy with stable central nervous system penetration score. *HIV Med* **14**, 311-315 (2013).
33. Caniglia, E.C., *et al.* Antiretroviral penetration into the CNS and incidence of AIDS-defining neurologic conditions. *Neurology* **83**, 134-141 (2014). PMCID PMC4117168.
34. Berger, J.R. & Clifford, D.B. The relationship of CPE to HIV dementia: slain by an ugly fact? *Neurology* **83**, 109-110 (2014).
35. Yuan, N.Y. & Kaul, M. Beneficial and Adverse Effects of cART Affect Neurocognitive Function in HIV-1 Infection: Balancing Viral Suppression against Neuronal Stress and Injury. *J Neuroimmune Pharmacol* (2019). PMCID PMC7233291.
36. Robertson, K., Liner, J. & Meeker, R.B. Antiretroviral neurotoxicity. *J Neurovirol* **18**, 388-399 (2012). PMCID PMC3581315.
37. Ciavatta, V.T., *et al.* In vitro and Ex vivo Neurotoxic Effects of Efavirenz are Greater than Those of Other Common Antiretrovirals. *Neurochem Res* **42**, 3220-3232 (2017).
38. Akay, C., *et al.* Antiretroviral drugs induce oxidative stress and neuronal damage in the central nervous system. *J Neurovirol* **20**, 39-53 (2014). PMCID PMC3928514.
39. Bond, S., Lopez-Lloreda, C., Gannon, P.J., Akay-Espinoza, C. & Jordan-Sciutto, K.L. The Integrated Stress Response and Phosphorylated Eukaryotic Initiation Factor 2alpha in

Neurodegeneration. *Journal of neuropathology and experimental neurology* **79**, 123-143 (2020). PMCID PMC6970450.

40. Gannon, P.J.*, et al.* HIV Protease Inhibitors Alter Amyloid Precursor Protein Processing via beta-Site Amyloid Precursor Protein Cleaving Enzyme-1 Translational Up-Regulation. *Am J Pathol* **187**, 91-109 (2017). PMCID PMC5225305.
41. Stern, A.L.*, et al.* Differential Effects of Antiretroviral Drugs on Neurons In Vitro: Roles for Oxidative Stress and Integrated Stress Response. *J Neuroimmune Pharmacol* **13**, 64-76 (2018). PMCID PMC5821494.
42. McDonough, P.M., Prigozhina, N.L., Basa, R.C.B. & Price, J.H. Assay of Calcium Transients and Synapses in Rat Hippocampal Neurons by Kinetic Image Cytometry and High-Content Analysis: An In Vitro Model System for Postchemotherapy Cognitive Impairment. *Assay Drug Dev Technol* **15**, 220-236 (2017). PMCID PMC5549836.
43. Xu, P.*, et al.* Combined Medication of Antiretroviral Drugs Tenofovir Disoproxil Fumarate, Emtricitabine, and Raltegravir Reduces Neural Progenitor Cell Proliferation In Vivo and In Vitro. *J Neuroimmune Pharmacol* **12**, 682-692 (2017). PMCID PMC5693968.
44. Demir, M. & Laywell, E.D. Neurotoxic effects of AZT on developing and adult neurogenesis. *Frontiers in neuroscience* **9**, 93 (2015). PMCID PMC4367529.
45. Pfeiffer, E.R., Vega, R., McDonough, P.M., Price, J.H. & Whittaker, R. Specific prediction of clinical QT prolongation by kinetic image cytometry in human stem cell derived cardiomyocytes. *J Pharmacol Toxicol Methods* **81**, 263-273 (2016).
46. Haralick, R.M. & Shanmugam, K. Textural features for image classification. *IEEE Transactions on systems, man, and cybernetics*, 610-621 (1973).
47. Hamilton, N.A., Pantelic, R.S., Hanson, K. & Teasdale, R.D. Fast automated cell phenotype image classification. *BMC Bioinformatics* **8**, 110 (2007). PMCID PMC1847687.
48. Farhy, C.*, et al.* Improving drug discovery using image-based multiparametric analysis of the epigenetic landscape. *Elife* **8**(2019). PMCID PMC6908434.
49. Schnoll, J.G.*, et al.* Evaluating Neurodevelopmental Consequences of Perinatal Exposure to Antiretroviral Drugs: Current Challenges and New Approaches. *J Neuroimmune Pharmacol* (2019). PMCID PMC7064402.
50. Ryan, S.K.*, et al.* Neuroinflammation and EIF2 Signaling Persist despite Antiretroviral Treatment in an hiPSC Tri-culture Model of HIV Infection. *Stem cell reports* **14**, 703-716 (2020). PMCID PMC7160309.
51. Shiau, S.*, et al.* Distinct epigenetic profiles in children with perinatally-acquired HIV on antiretroviral therapy. *Scientific reports* **9**, 10495 (2019). PMCID PMC6642153.

Figure 1

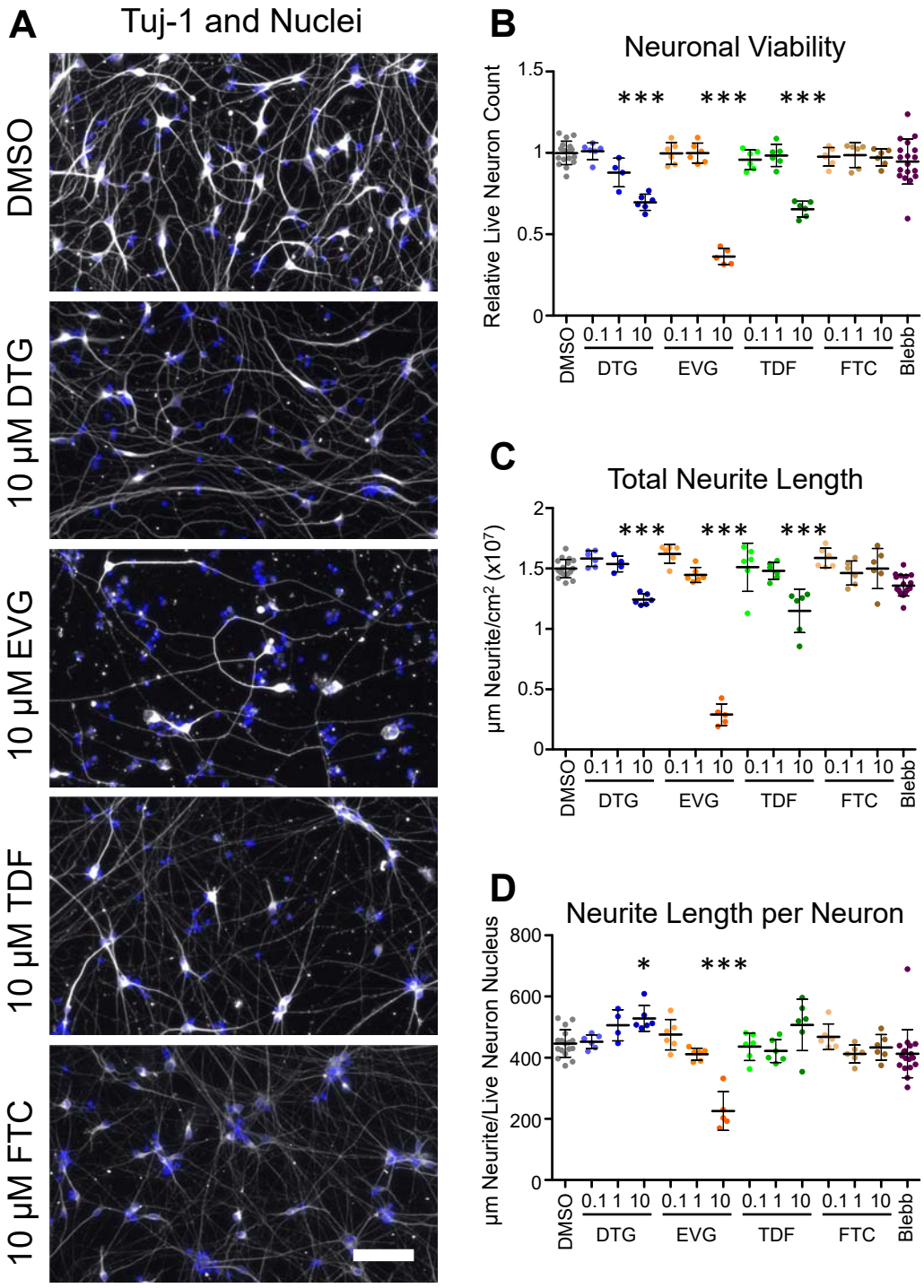

Figure 2

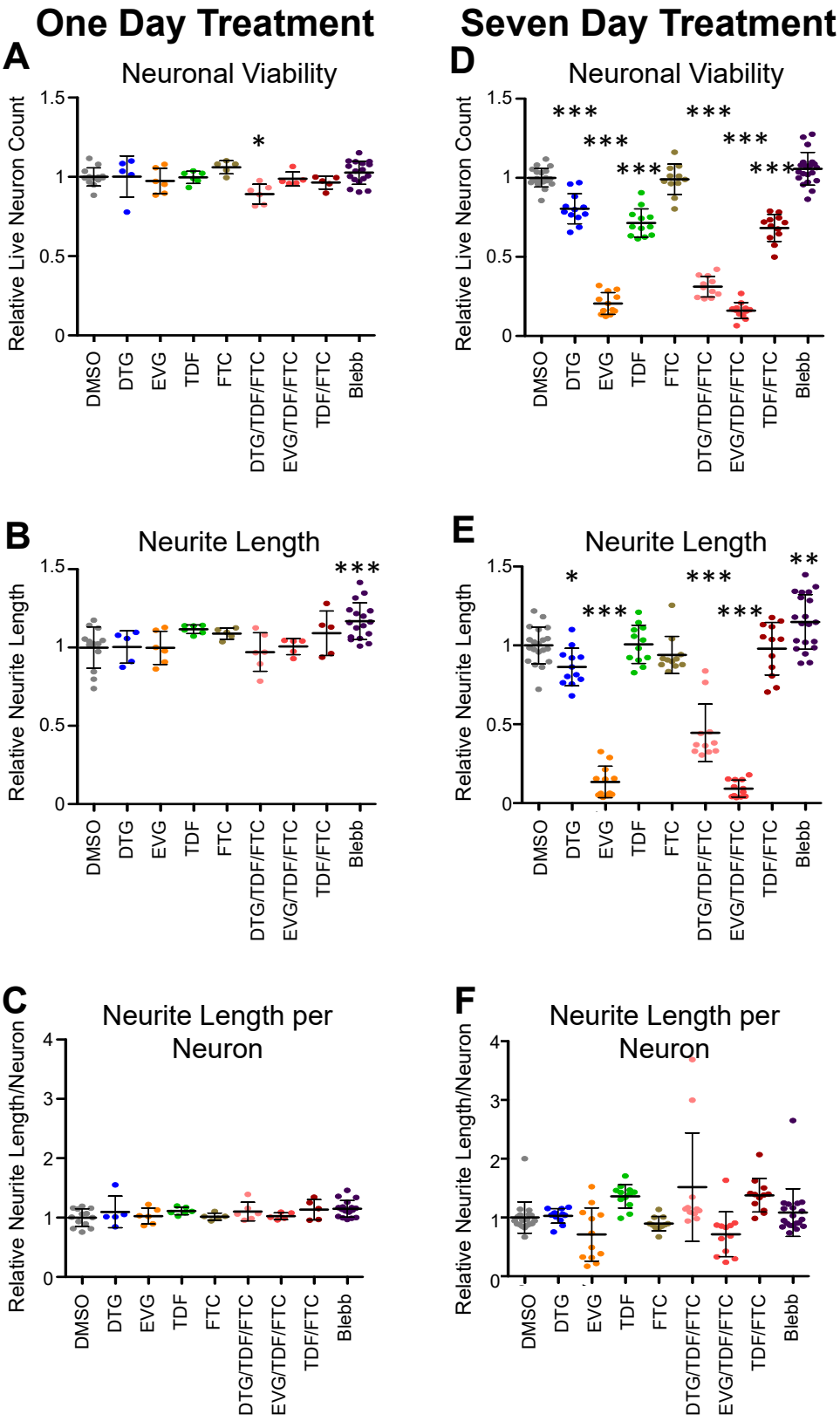

Figure 3

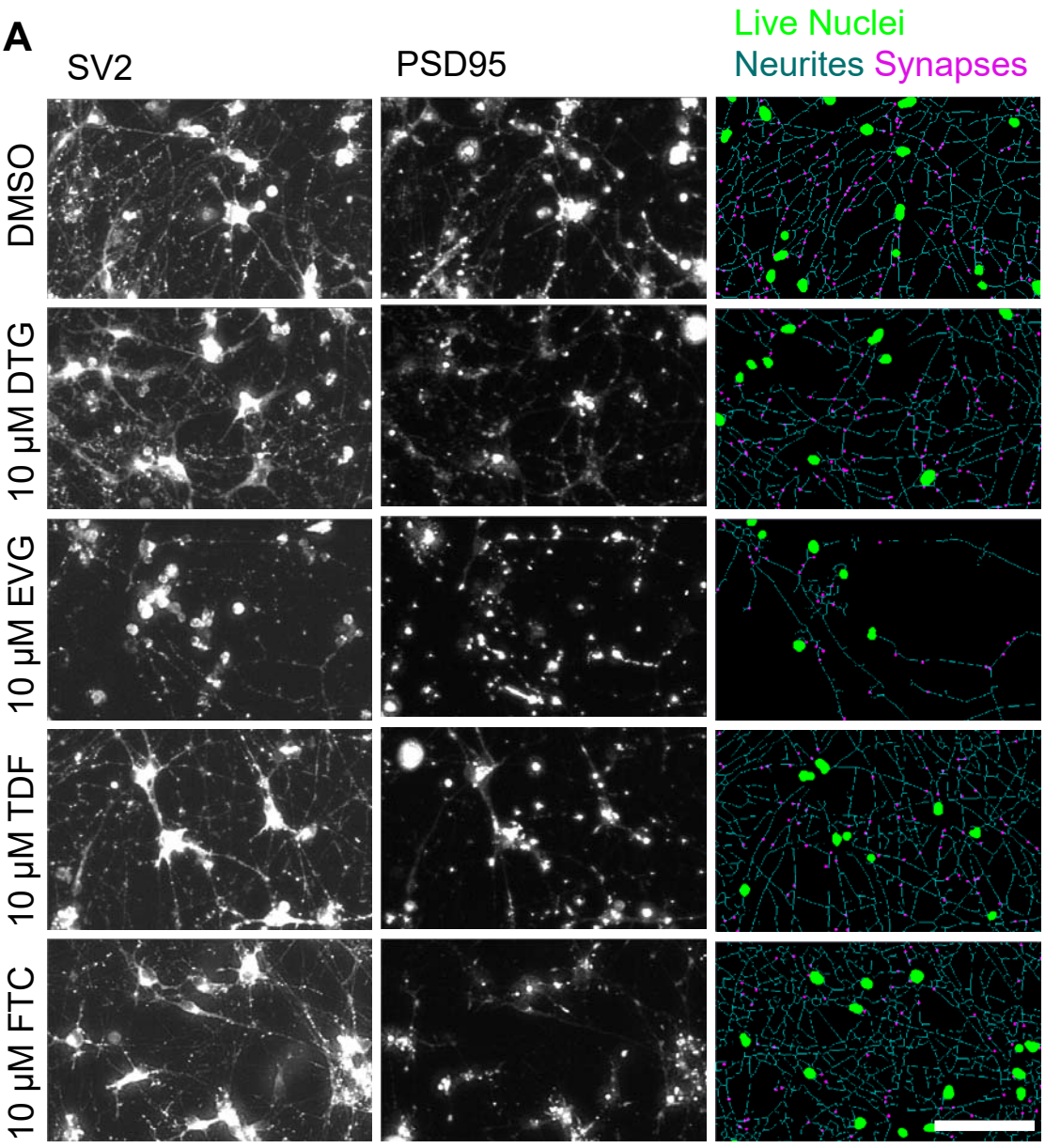

Figure 4

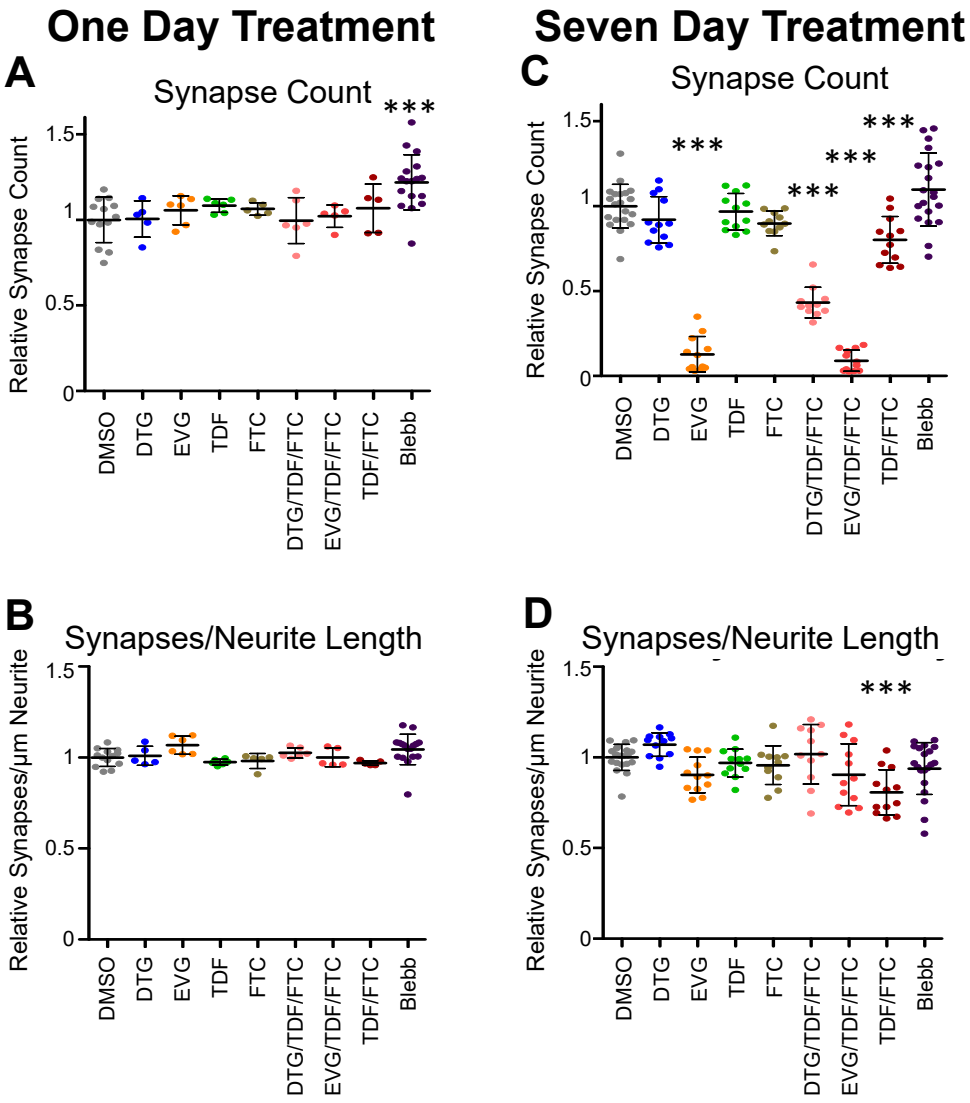

Figure 5

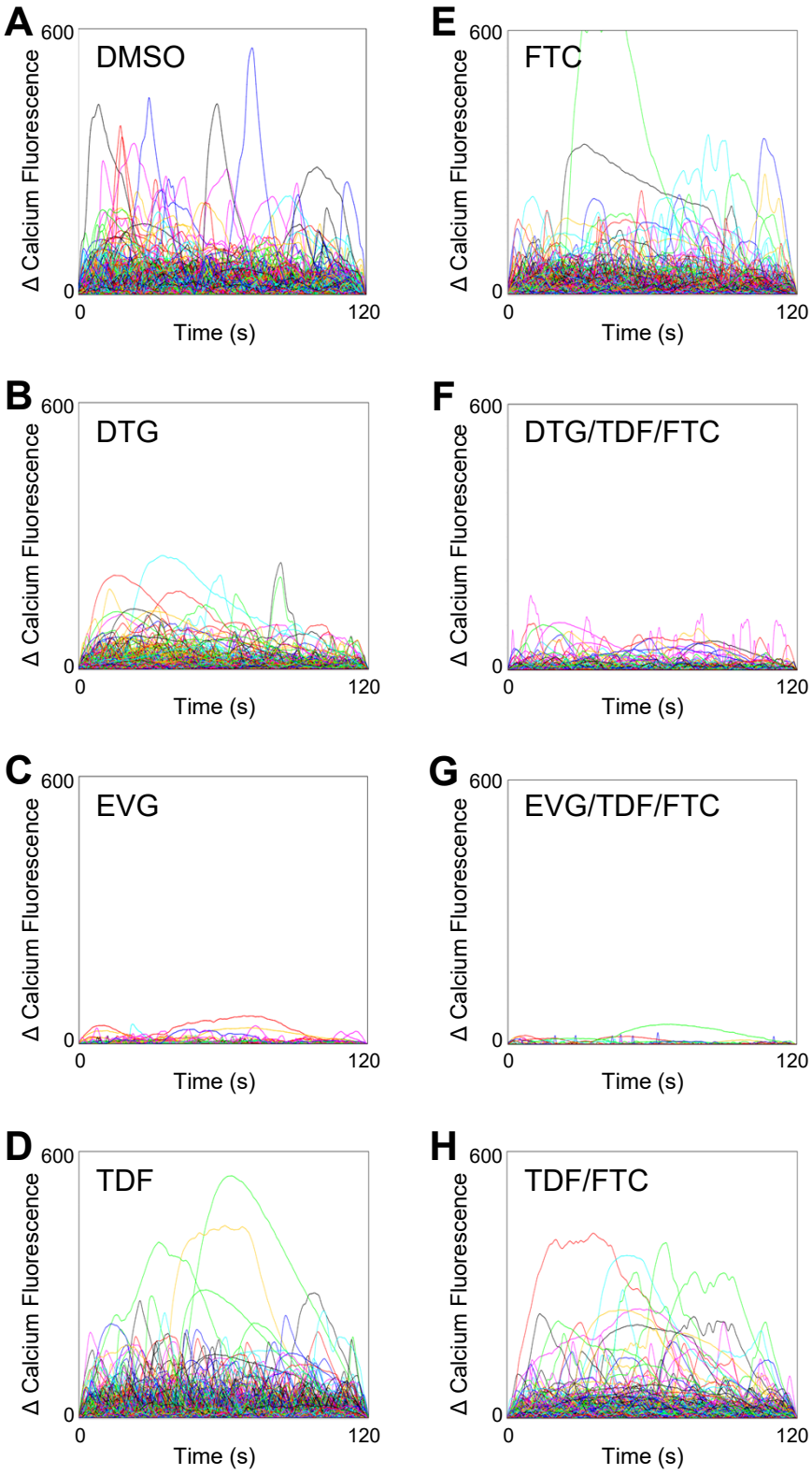

Figure 6

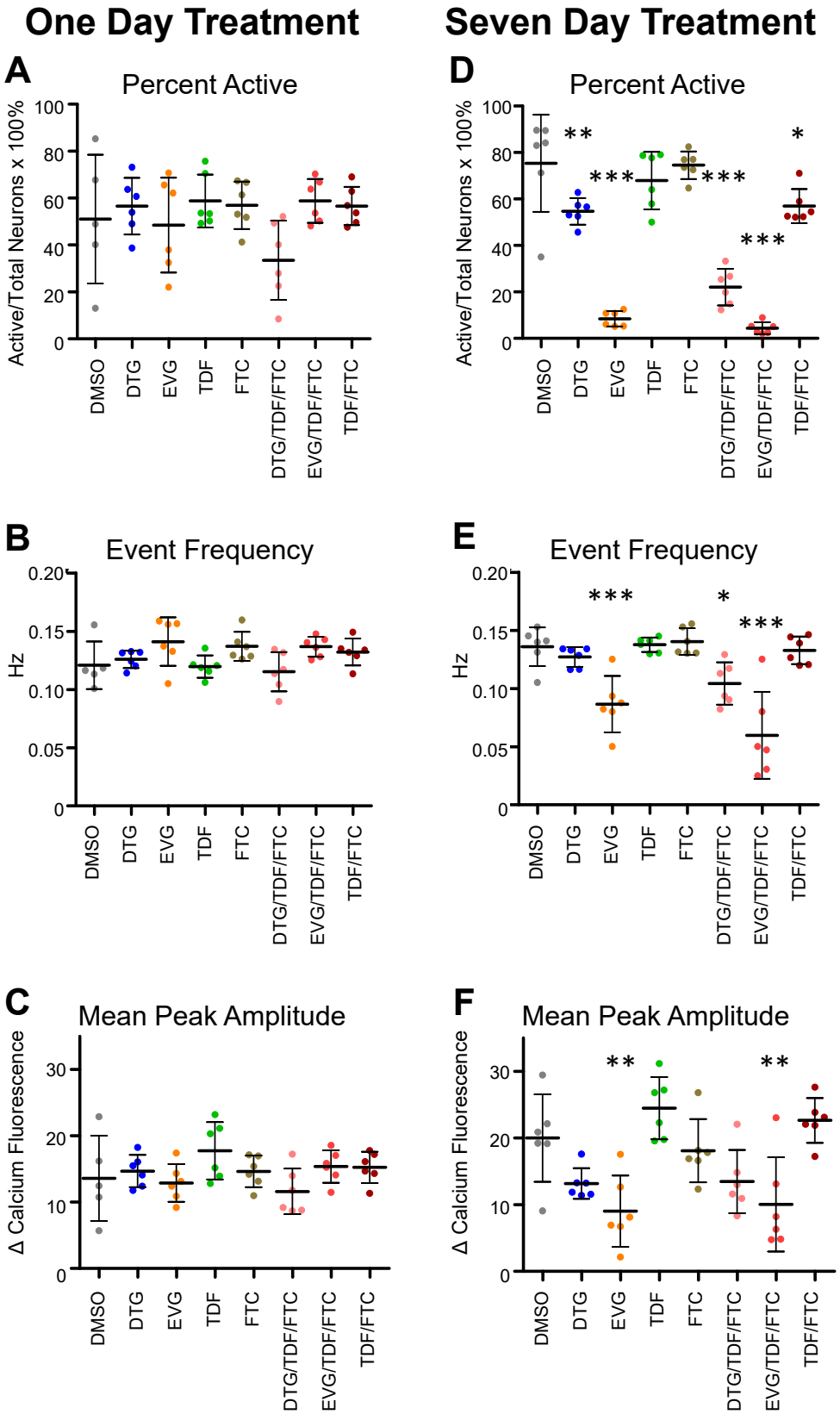

Figure 7

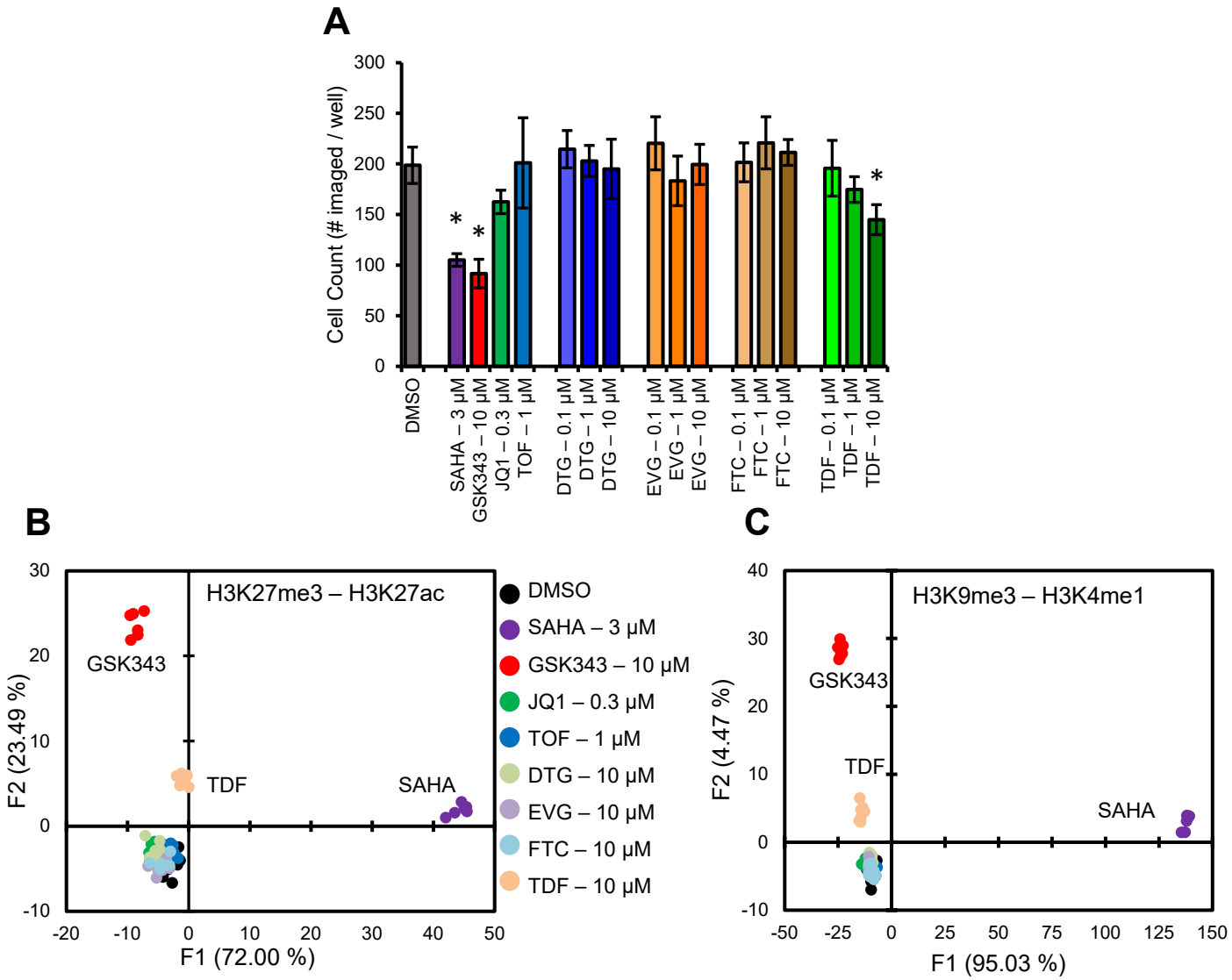

D

	DMSO	GSK343 - 10uM	SAHA - 3uM	JQ1 - 0.3uM	TOF - 1uM	DTG - 10uM	EVG - 10uM	FTC - 10uM	TDF - 10uM
DMSO	33.3	0.0	0.0	0.0	16.7	16.7	16.7	16.7	0.0
GSK343 - 10uM	0.0	100.0	0.0	0.0	0.0	0.0	0.0	0.0	0.0
SAHA - 3uM	0.0	0.0	100.0	0.0	0.0	0.0	0.0	0.0	0.0
JQ1 - 0.3uM	0.0	0.0	0.0	33.3	0.0	0.0	33.3	33.3	0.0
TOF - 1uM	33.3	0.0	0.0	0.0	0.0	0.0	0.0	66.7	0.0
DTG - 10uM	66.7	0.0	0.0	0.0	0.0	0.0	0.0	33.3	0.0
EVG - 10uM	33.3	0.0	0.0	33.3	0.0	33.3	0.0	0.0	0.0
FTC - 10uM	33.3	0.0	0.0	0.0	0.0	33.3	0.0	33.3	0.0
TDF - 10uM	0.0	0.0	0.0	0.0	0.0	0.0	0.0	0.0	100.0

E

	DMSO	GSK343 - 10uM	SAHA - 3uM	JQ1 - 0.3uM	TOF - 1uM	DTG - 10uM	EVG - 10uM	FTC - 10uM	TDF - 10uM
DMSO	83.3	0.0	0.0	0.0	0.0	16.7	0.0	0.0	0.0
GSK343 - 10uM	0.0	100.0	0.0	0.0	0.0	0.0	0.0	0.0	0.0
SAHA - 3uM	0.0	0.0	100.0	0.0	0.0	0.0	0.0	0.0	0.0
JQ1 - 0.3uM	33.3	0.0	0.0	33.3	33.3	0.0	0.0	0.0	0.0
TOF - 1uM	0.0	0.0	0.0	0.0	0.0	33.3	33.3	33.3	0.0
DTG - 10uM	25.0	0.0	0.0	0.0	0.0	25.0	25.0	25.0	0.0
EVG - 10uM	50.0	0.0	0.0	0.0	0.0	0.0	50.0	0.0	0.0
FTC - 10uM	0.0	0.0	0.0	0.0	0.0	25.0	50.0	25.0	0.0
TDF - 10uM	0.0	0.0	0.0	0.0	0.0	0.0	0.0	0.0	100.0